

# Early Voltage and Current Gain of $\text{Si}_{1-y}\text{Ge}_y$ Heterojunction Bipolar Transistor

Fazle Rabbi, Yeasir Arafat\*, M. Ziaur Rahman Khan

Department of EEE, BUET, Dhaka, 1000, Bangladesh

**Abstract** Closed form analytical models were derived for Early voltage ( $V_A$ ) and common emitter current gain ( $\beta$ ) for  $\text{Si}_{1-y}\text{Ge}_y$  Heterojunction Bipolar Transistor (HBT). Field dependent mobility, doping dependent mobility, band gap narrowing (BGN) effect (due to both heavy doping and presence of Germanium content in the base) and velocity saturation effects were considered in these models. The derived models are applicable for uniform, exponential and Gaussian types of base doping profiles and trapezoidal, triangular or box germanium profiles. The variations of  $V_A$ ,  $\beta$ , intrinsic carrier concentration, diffusivity and electric field in the base region with the variation of germanium mole fraction were studied. The results obtained by these analytical models were compared with the results available in the literature and found in good agreement.

**Keywords** Early Voltage and Current Gain, Field Dependent Mobility, Gaussian Profile, SiGe base HBT

## 1. Introduction

Heterojunction Bipolar Transistor (HBT) is the outcome of extensive research on Bipolar Junction Transistor (BJT). Heterojunction Bipolar Transistor devices offer a number of advantages over their homo junction counterparts; in particular, SiGe-base HBTs are efficient alternative to III-V HBTs. Its use in very high frequency application is significant[1]. Bandgap engineering on silicon device can be done by Silicon Germanium (SiGe) HBT. Extremely high values of the emitter efficiency and additional degree of freedom in device design are possible because of a narrow-gap material in the base region. By introducing compositional grading in the base region further improvements in device performance can be achieved[2]. The Ge introduced into the base region reduces the band gap in the base, compared to that in Si BJT [3].

Device characteristics of HBT are defined by two very significant parameters like  $V_A$  and  $\beta$ [4]. When base grading creates bandgap at the base-collector junction lower than maximum bandgap, it will increase  $V_A$  and hence  $\beta V_A$  product which is an important Figure of merit[5]. Many works have been done to calculate  $V_A$  and  $\beta$ . Tadao fabricated AlGaAs/GaAs/AlGaAs structure HBT and studied  $V_A$  and  $\beta$  for this structure[6]. Tang et al. derived a closed form analytical model of  $V_A$  and  $\beta$  for a uniform doped base HBT with very thin Si emitters[5].

The effect of surface recombination of AlGaAs/GaAs/

AlGaAs HBT on the  $V_A$  was studied by Chiu et al.[7]. This model did not consider the effect of electric field on mobility while calculating  $V_A$ . Effect of Ge content at the collector base junction on  $V_A$  was investigated by Dong et al.[8]. At high doping concentration and high Ge content, neutral baserecombination effect on  $\beta$  were analysed by Ningyue et al. for uniform base doping profile[9]. Prinz et al. studied  $V_A$  and  $\beta$  in HBT where bandgap varies across the base[10]. This model is applicable for uniformly doped base and the effect of velocity saturation and field dependent diffusivity were neglected in this model. Yuan et al. modified Prinz's works by including neutral base re-combination effect on  $V_A$ [11]. Early voltage improvement using deep sub-micron technique was proposed by Conrad et al[12]. Modelling and improvement of current gain for a uniform doped base SiC power bipolar junction transistor was done by Domeij [13]. A new bipolar junction transistor for enhanced current gain and reduced hot carrier degradation was proposed by Kumar et al. [14]. Ge content in the base as well as heavy base doping cause BGN[15]. So BGN due to heavy doping should consider while calculating  $V_A$  and  $\beta$ . Zareba derived a new model of  $V_A$  considering field dependent diffusivity, velocity saturation and band gap narrowing effects for Gaussian doped base HBT[16]. This model was not in closed form and it was done only for triangular germanium profile in the base. Babcock et al. have done a comprehensive investigation of temperature dependence of current gain ( $\beta$ ) and Early voltage ( $V_A$ ) for SiGe-npn transistors[17]. Babcock et al. also done comprehensive investigation of Early voltage ( $V_A$ ) versus drive current dependence for SiGe-pnp bipolar transistors fabricated on thick-film SOI[18]. Ziao B. et al. generalized SGP model of standard Early voltage for SiGe-npn heterojunction bipolar transistors (HBTs)[19]. A com-

\* Corresponding author:

arafat@eee.buet.ac.bd (Yeasir Arafat)

Published online at <http://journal.sapub.org/msse>

Copyright © 2012 Scientific & Academic Publishing. All Rights Reserved

plete closed form analytical model of  $V_A$  and  $\beta$  for HBT with different base doping profile (uniform, exponential and Gaussian) and trapezoidal/triangular/box germanium profile in the base is yet to be reported where the necessary effects were considered.

In this work, a new model for Early voltage ( $V_A$ ) and common emitter current gain ( $\beta$ ) were derived for three different base doping profiles (Gaussian, exponential and uniform) and Germanium profiles (trapezoidal, triangular and box). Germanium profile incorporate band gap engineering in silicon base. A model for effective intrinsic carrier concentration ( $n_{ieSiGe}$ ), diffusivity ( $D_{nSiGe}$ ), electric field ( $E_{lSiGe}$ ), collector saturation current ( $J_{CO}$ ) were derived for SiGe HBT considering field dependent mobility, BGN and velocity saturation effect. These parameters were used to explain the variation of  $V_A$  and  $\beta$  for various base doping profiles and germanium profiles.

## 2. Analysis

For arbitrary doped base HBT with arbitrary Ge profile, the collector saturation current density can be expressed as [20].

$$J_{CO} = \frac{q}{\int_0^{W_B} \frac{N_B(x)}{n_{ieSiGe}^2(x) D_{nSiGe}(x)} dx + \frac{N_B(W_B)}{n_{ieSiGe}^2(W_B) v_{sA}}} \quad (1a)$$

where,  $D_{nSiGe}$ ,  $n_{ieSiGe}$  and  $J_{CO}$  are the electron diffusion coefficient, effective intrinsic carrier concentration and collector saturation current density in SiGe HBT respectively.  $N_B(x)$  is the base doping profile,  $x$  is the length along base,  $W_B$  is the base width and  $v_{sA}$  is the saturation velocity within the alloy,  $q$  is the charge of electron.  $N_B(W_B)$  and  $n_{ieSiGe}(W_B)$  is doping concentration and effective intrinsic carrier concentration at base-collector junction respectively.

The common emitter current gain ( $\beta$ ) can be found from equation (1a)

$$\beta = \frac{J_{CO}}{J_{BO}} = \frac{q/J_{BO}}{\int_0^{W_B} \frac{N_B(x)}{n_{ieSiGe}^2(x) D_{nSiGe}(x)} dx + \frac{N_B(W_B)}{n_{ieSiGe}^2(W_B) v_{sA}}} \quad (1b)$$

where,  $J_{BO}$  is the base saturation current density.

Generally the early voltage is defined as [16]

$$V_A = J_C \left( \frac{\delta W_B}{\delta J_C} \cdot \frac{\delta V_{BC}}{\delta W_B} \right) \quad V_{BE} = \text{constant} \quad (2a)$$

where,  $V_{BC}$  is the base to collector voltage,  $V_{BE}$  is base-emitter voltage.  $\delta J_C$  is the collector current variation due to change in  $V_{BC}$  ( $\delta V_{BC}$ ).

The early voltage can be derived by solving equation (1a) and (2a) and is given by:

$$V_A = \frac{q n_{ieSiGe}^2(W_B) D_{nSiGe}(W_B)}{C_{BC}} \times \left( \int_0^{W_B} \frac{N_B(x)}{n_{ieSiGe}^2(x) D_{nSiGe}(x)} dx + \frac{N_B(W_B)}{n_{ieSiGe}^2(W_B) v_{sA}} \right) \quad (2b)$$

where,  $C_{BC}$  is the base-collector junction capacitance.

From equation (1b) and (2b), product of current gain-early voltage ( $\beta V_A$ ) becomes

$$\beta V_A = \frac{q^2 n_{ieSiGe}^2(W_B) D_{nSiGe}(W_B)}{J_{BO} C_{BC}} \quad (3)$$

The Ge mole fraction ( $y$ ) distribution profiles of an npnSiGe-base HBT is shown in Fig 1. For a trapezoidal profile,  $y$  can be expressed as a function of distance ( $x$ ) along the neutral base width  $W_B$ , as

$$y(x) = m_{Ge} x + y_E \quad (4)$$

where  $m_{Ge} = \eta_{Ge}/W_B$ ;  $\eta_{Ge} = y_C - y_E$ ;  $y_C$  and  $y_E$  are Ge fraction at the base-collector junction and base-emitter junction respectively. For  $y_E = 0$ , (4) represents triangular profile, for  $y_E = y_C$ , (4) represents box shape profile.

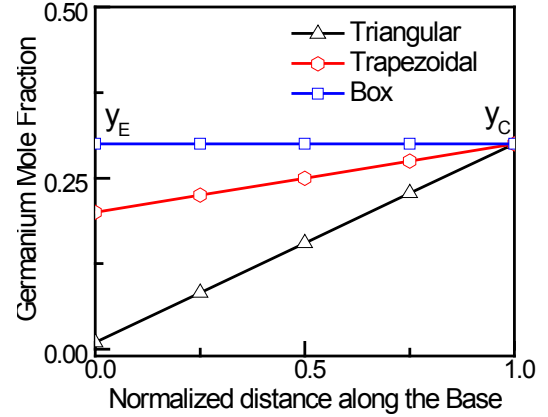


Figure 1. Germanium profile in SiGe HBT

The electric field equation within the base region can be written as

$$E_{SiGe}(x) = \frac{kT}{q} \left( \frac{1}{p(x)} \frac{dp(x)}{dx} - \frac{1}{n_{ieSiGe}^2(x)} \frac{dn_{ieSiGe}^2(x)}{dx} \right) \quad (5)$$

where,  $k$  is the Boltzmann constant and  $T$  is the temperature in degrees Kelvin.

The electron diffusion length in silicon is about 500 nm [21]. The carrier recombination in the base region can safely be neglected for today's HBT as the base width is less than 100nm [22].

Base doping profile for uniform, exponential and Gaussian are given by (6a), (6b) and (6c) respectively:

$$N_B(x) = N_B(0) \quad (6a)$$

$$N_B(x) = N_B(0) e^{-m_{exp} x} \quad (6b)$$

$$N_B(x) = N_B(0) e^{-m_{gauss} x^2} \quad (6c)$$

$$m_{exp} = \frac{\ln(N_B(0)/N_B(W_B))}{W_B} \quad (7a)$$

$$m_{gauss} = \frac{\ln(N_B(0)/N_B(W_B))}{W_B^2} \quad (7b)$$

$N_B(0)$  and  $N_B(W_B)$  are the peak doping concentration at the base-emitter and base-collector junction respectively.

Diffusivity equation can be written for impurity doping in Si base [23]:

$$D_{nSi}(x) = D_n \quad (8a)$$

$$D_{nSi}(x) = D_n e^{m_{1exp} x} \quad (8b)$$

$$D_{nSi}(x) = D_n e^{m_{1gauss} x^2} \quad (8c)$$

Equation (8a), (8b) and (8c) represents diffusion coefficient for uniform, exponential and Gaussian base doping profile respectively, where

$$D_n = D_{no} \left( \frac{N_B(0)}{N_r} \right)^{-\gamma_1}, \quad D_{no} = \frac{20.72 \text{ cm}^2}{s},$$

$$N_r = 10^{17} \text{ cm}^{-3} m_{1exp} = m_{exp} \gamma_1,$$

$$m_{1gauss} = m_{gauss} \gamma_1 \text{ and } \gamma_1 = 0.42..$$

Now Electron diffusivity in the presence of Germanium is [24]

$$D_{nSiGe}(x) = b D_{nSi}(x) \quad (9)$$

$$\text{where, } b = 1 + 3\gamma_{av}, \gamma_{av} = \frac{\gamma_C + \gamma_E}{2}.$$

The saturation velocity inside the SiGe alloy differs from that in Si and is given by [25]

$$v_{sa} = c v_s \quad (10a)$$

$$\text{where, } v_s = 10^7 \text{ cm/s, } c = \frac{0.342}{0.342 + \gamma_{av}(1 - \gamma_{av})} \quad (10b)$$

The expression for field dependent mobility,  $\mu_n(E)$  is an empirical one and can be shown as [26]

$$\mu_{nSi}(E) = \frac{v_s}{a|E(x)| + E_{cSi}(x)} \quad (11a)$$

where,  $a = 0.7743$ ;  $E_{cSi}(x)$  is the critical electric field

$$E_{cSi}(x) = \frac{v_s}{\mu_{nSi}(x)} \quad (11b)$$

Using equations (9)-(11b), Einstein relation and considering electric field dependency, diffusion coefficient in Silicon Germanium base can be written as

$$D_{nSiGe}(x) = \frac{b v_s D_{nSi}(x)}{(a|E_{SiGe}(x)| D_{nSi}(x) + v_s)} \quad (12)$$

The effective intrinsic concentration in SiGe is [24]

$$n_{ieSiGe}^2(x) = (x) n_{ioSi}^2 \cdot e^{\frac{\Delta E_{geff}(x)}{kT}} \quad (13)$$

where  $(x)$  is the ratio of the effective density of states in SiGe to the effective density of states in silicon and given by [27].

$$(x) = \exp(-\sqrt{5} \gamma(x)) \quad (14)$$

$n_{ioSi} = 1.4 \times 10^{10} \text{ cm}^{-3}$  is the intrinsic carrier concentration in silicon.

$\Delta E_{geff}(x)$  is the effective bandgap reduction in the SiGe base that can be expressed as

$$\Delta E_{geff}(x) = \Delta E_{gHD}(x) + \Delta E_{gGe}(x) \quad (15)$$

where,  $\Delta E_{gGe}(x)$  is the BGN due to the presence of Ge which is assumed to have a linear dependence on Ge concentration;  $\Delta E_{gHD}(x)$  is the BGN due to heavy doping effects and is identical to that of silicon. An approximation of the Slotboom-de Graff BGN model [28] is used for this term

$$\Delta E_{gHD}(x) = q V_{gHD} \ln \left( \frac{N_B(x)}{N_r} \right) \quad (16)$$

with,  $V_{gHD} = 18 \text{ mV}$  and the BGN due to the presence of Ge is given by [29]

$$\Delta E_{gGe}(x) = q V_{gGe} \gamma(x) \quad (17)$$

with,  $V_{gGe} = 688 \text{ mV}$ .

Using equations (13)-(17), effective intrinsic concentration in SiGe can be expressed as:

$$n_{ieSiGe}^2(x) = n_{ioSi}^2 e^{3\gamma_e \left( \frac{N_B(0)}{N_r} \right)^2} e^{(m_3 x - m_2 x^\alpha)} \cdot (x) \quad (18)$$

where,  $2 = V_{gHD}/V_T = 0.69$ ,  $3 = V_{gGe}/V_T = 26.37$ ,  $m_3 = 3$ ,  $m_{Ge}$ ,  $m_2$  for uniform, exponential and Gaussian based doped will be 0,  $m_{exp-2}$  and  $m_{gauss-2}$  respectively.  $\alpha$  for uniform, exponential and Gaussian doped base will be 0, 1 and 2 respectively.

The quasi neutrality of charge within the base of a bipolar transistor will be  $p(x) = n(x) + N_B(x)$ . Considering low injection,  $p(x) = N_B(x)$  and putting equation (18) in (5), the

electric field equation for low injection will be:

$$E_{SiGe}(x) = V_T \left( m_3 + 0.31 \alpha m x^{(\alpha-1)} - \left( \frac{m_{Ge} \sqrt{5}}{2} \right) \frac{1}{\sqrt{m_{Ge} x + \gamma_E}} \right) \quad (19)$$

Value of  $m$  for uniform, exponential and Gaussian will be 0,  $m_{exp}$  and  $m_{gauss}$  respectively. Equation (19) is used to calculate  $D_{nSiGe}$  in equation (12). By using the value of  $D_{nSiGe}$ ,  $n_{ieSiGe}^2$  and  $E_{SiGe}(x)$  from equation (12), (18) and (19) respectively we can find  $\beta$  and  $V_A$  from (1b) and (2b) respectively.

Deriving the closed loop form of  $V_A$  and  $\beta$ , ratio of effective density of states in SiGe to the effective density of states in silicon was considered fixed throughout the base region [27].

$$(x) = r = \exp(-\sqrt{5} \gamma_{av}) \quad (20)$$

Considering equation (20), equation (18) and (19) minimize to (21) and (22) respectively.

$$n_{ieSiGe}^2(x) = n_{ieSiGe}^2(0) \cdot e^{(m_3 x - m_2 x^\alpha)} \quad (21)$$

$$\text{where, } n_{ieSiGe}^2(0) = n_{ioSi}^2 e^{-3\gamma_e \left( \frac{N_B(0)}{N_r} \right)^2} \cdot r$$

$$E_{SiGe}(x) = V_T (m_3 + 0.31 \alpha m x^{(\alpha-1)}) \quad (22)$$

By using equations (12), (21) and (22) in (2b)  $V_A$  for Gaussian doped base can be derived as:

$$V_A = \left( I_1 + \frac{N_B(W_B)}{n_{ieSiGe}^2(W_B) \cdot v_{sA}} \right) \left( \frac{q n_{ieSiGe}^2(W_B)}{C} \right) \times \left( \frac{b v_s D_n e^{m_1 W_B}}{v_s + a(m_3 + 0.62 m W_B) D_n e^{m_1 W_B}} \right) \quad (23)$$

where

$$I_1 = \frac{a N_B(0) e^{-\frac{m_2^2}{4(m_2 - m_1)}}}{b v_s n_{ieSiGe}^2(0) 4(m_2 - m_1)^2} \left[ \sqrt{\pi} (2m_2(m_2 - m_1) + 0.62 m m_2) \left\{ \operatorname{erfi} \left( \frac{-m_3 + 2(m_2 - m_1) W_B}{2\sqrt{(m_2 - m_1)}} \right) - \operatorname{erfi} \left( \frac{-m_3}{2\sqrt{(m_2 - m_1)}} \right) \right\} \right. \\ \left. + 1.24 m \sqrt{(m_2 - m_1)} e^{\frac{(-m_3 + 2(m_2 - m_1) W_B)^2}{4(m_2 - m_1)}} - e^{\frac{m_2^2}{4(m_2 - m_1)}} \right] \\ + \frac{N_B(0) \sqrt{\pi} e^{-\frac{m_2^2}{4(m_2 - m_1)}}}{2b D_n n_{ieSiGe}^2(0) (m_2 - m_1 - m)^2} \left\{ \operatorname{erfi} \left( \frac{-m_3 + 2(m_2 - m_1 - m) W_B}{2\sqrt{(m_2 - m_1 - m)}} \right) - \operatorname{erfi} \left( \frac{-m_3}{2\sqrt{(m_2 - m_1 - m)}} \right) \right\} \quad (24)$$

By using equations (12), (21) and (22) in (1b)  $\beta$  for Gaussian doped base can be derived as:

$$\beta = \frac{J_{CO}}{J_{BO}} = \frac{q/J_{BO}}{I_1 + \frac{N_B(W_B)}{n_{ieSiGe}^2(W_B) v_{sA}}} \quad (25)$$

where,  $I_1$  can be found from (24)

In the same way  $V_A$  for exponential doped base can be found:

$$V_A = \left( I_2 + \frac{N_B(W_B)}{n_{ieSiGe}^2(W_B) \cdot v_{sA}} \right) \left( \frac{q n_{ieSiGe}^2(W_B)}{C} \right) \left( \frac{b v_s D_n e^{m_1 W_B}}{v_s + a m_{032} D_n e^{m_1 W_B}} \right) \quad (26)$$

where,

$$I_2 = \frac{N_B(0) a m_{032}}{n_{ieSiGe}^2(0) b v_s m_{132}} (1 - e^{-m_{132} W_B})$$

$$+ \frac{N_B(0)}{n_{ieSiGe}^2(0)bD_n m_{0132}} (1 - e^{-m_{0132} W_B}) \quad (27)$$

and,  $m_{32}=m_3-m_2$ ,  $m_{032}=m+m_3-m_2$ ,  $m_{132}=m_1+m_{32}$ ,  $m_{0132}=m+m_1+m_{32}$ .

$\beta$  for exponential doped base can be found by putting  $I_2$  instead of  $I_1$  in (25)

$V_A$  for uniform doped base will be:

$$V_A = \left( I_3 + \frac{N_B(0)}{n_{ieSiGe}^2(W_B) \cdot v_{sA}} \right) \left( \frac{q n_{ieSiGe}^2(W_B)}{C} \right) \left( \frac{b v_s D_n}{a m_3 D_n + v_s} \right) \quad (28)$$

$$\text{where, } I_3 = \frac{N_B(0)(a m_3 D_n + v_s)}{n_{ieSiGe}^2(0) b v_s D_n m_3} (1 - e^{-m_3 W_B}) \quad (29)$$

$\beta$  for uniform doped base can be found by putting  $I_3$  instead of  $I_1$  in (25).

### 3. Result and Discussion

The calculation is done for an HBT with 300Å base width. Base doping at the base emitter junction is  $10^{19} \text{ cm}^{-3}$  and at base-collector junction is  $10^{17} \text{ cm}^{-3}$  for Gaussian and exponential doped base and  $10^{19} \text{ cm}^{-3}$  was considered for uniform doped base. The base-collector junction capacitance assumed  $C_{BC} \approx 55 \text{ nF/cm}^2$  [10].

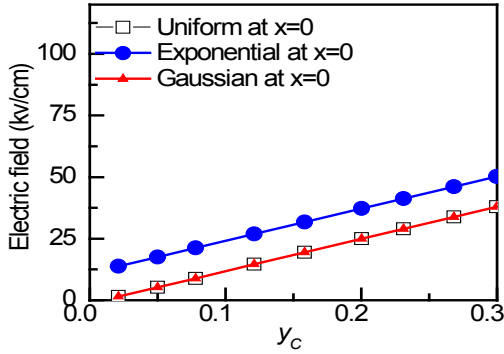


**Figure 2a.** Electric field at base-emitter junction,  $E_{iSiGe}(0)$  for  $y_E=0.01$  and varying  $y_C$  for three types of doping profiles

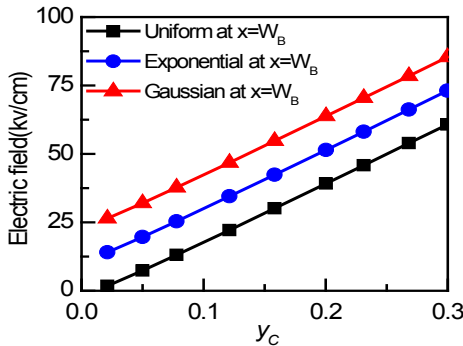
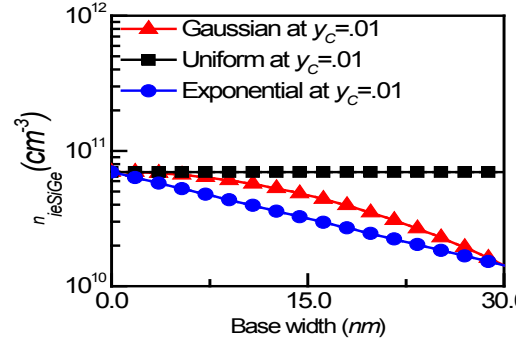


**Figure 2b.** Electric field at base-collector junction,  $E_{iSiGe}(W_B)$  for  $y_E=0.01$  and varying  $y_C$  for three types of doping profiles

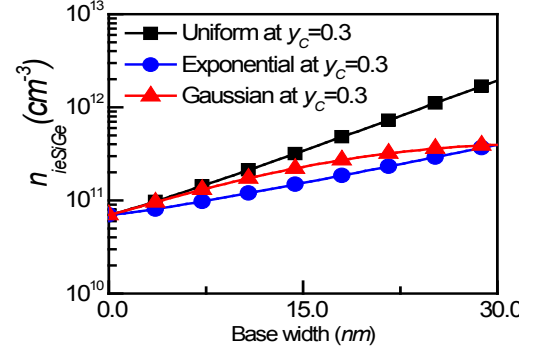
#### 3.1. Electric Field Profile

Figure 2a and Figure 2b shows that the electric field increases with  $y_C$ . Figure 2a shows electric field at base emitter junction and Figure 2b shows electric field at base collector junction. Increased Germanium will enhance BGN ( $\Delta E_{geff}$ ) which will increase effective intrinsic carrier concentration ( $n_{ieSiGe}$ ) exponentially (Figure 4). From equation (5) it can be observed that electric field reduces with the amount of base doping concentration and intrinsic carrier concentration but

it increases with the variation of base doping concentration and intrinsic carrier concentration variation. For uniformly doped base, doping concentration made 100 times than that of exponential and Gaussian doped base in this analysis, also intrinsic carrier concentration is much more than exponential and Gaussian base (Figure 3). But due to no variation of doping concentration and intrinsic concentration for uniform doped base electric field is lowest in comparison to exponential and Gaussian doped base at collector end. On the other hand at emitter end, base doping concentration ( $N_B$ ) and  $n_{ieSiGe}$  are same for all types of profile but variation of base doping is much more for exponential doped base in comparison to other two profiles, so electric field is much higher for exponential doped base.



**Figure 3a.** Intrinsic carrier concentration through the base for uniform, exponential and Gaussian doped base for both  $y_C$  and  $y_E$  at 0.01



**Figure 3b.** Intrinsic carrier concentration through the base for uniform, exponential and Gaussian doped base for  $y_C=0.3$  and  $y_E=0.01$

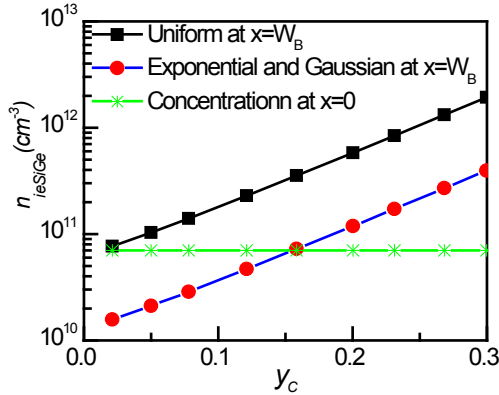
#### 3.2. Effective Intrinsic Carrier Concentration Profile

Figure 3a and Figure 3b shows distribution of effective intrinsic carrier concentration ( $n_{ieSiGe}$ ) throughout the base region for uniform, exponential and Gaussian doped profile. This distribution was plotted for two  $y_C$  value, one for  $y_C=0.01$  (Figure 3a) and other for  $y_C=0.3$  (Figure 3b). In both cases,  $y_E$  remain 0.01. For  $y_C=0.01$ , it is observed that  $n_{ieSiGe}$  profile exactly follows their respective base doping profile.

From Figure 3b, it is observed that for  $y_C=0.3$ ,  $n_{ieSiGe}$  increases for all three types of base doping profile. The concentration of  $n_{ieSiGe}$  near the base-collector junction is highest for uniformly doped base. Though the concentration of  $n_{ieSiGe}$  is same at base-collector and base-emitter junction for exponential and Gaussian doped base but it is not same between these two junctions. Actually  $n_{ieSiGe}$  is proportional to

base doping concentration and germanium content in the base.

Figure 4 shows effective intrinsic carrier concentration ( $n_{ieSiGe}$ ) at base-emitter junction and base-collector junction for three types of base doping profile (uniform, exponential and Gaussian). Here  $y_E$  is kept fixed at 0.01 and  $y_C$  is varied. It can be observed that for uniform doped base with increasing of  $y_C$ ,  $n_{ieSiGe}$  increases at the base-collector junction exponentially but at base-emitter junction it has no changes. The value of  $n_{ieSiGe}$  at both junctions is same while  $y_C$  is low (0.01). For exponential and Gaussian doped base  $n_{ieSiGe}$  also increases exponentially with  $y_C$  at base-collector junction but it remains same at base-emitter junction.  $n_{ieSiGe}$  is smaller at base-collector junction than base-emitter junction while  $y_C = y_E = 0$ . Though the concentration of  $n_{ieSiGe}$  is same at base-collector junction for exponential and Gaussian doped base and also same at base-emitter junction for these two profiles, but it is not same between the two junctions throughout the base region (Fig. 3a and Fig. 3b). Although BGN for all three types of profiles is same at base-collector junction for each  $y_C$ ,  $n_{ieSiGe}$  is greater for uniform doped base than other two profiles due to only difference in base doping concentration. At base-emitter junction  $n_{ieSiGe}$  is always same because base doping and BGN both are same at this junction for all three types of profiles. It can be observed from Fig. 4 that by increasing  $y_C$  from 0 to 0.3 without increasing  $N_B$  which results about fifteen times more  $n_{ieSiGe}$ . It can also be observed that by increasing  $N_B$  hundred times without increasing  $y_C$  which results  $n_{ieSiGe}$  to be increased by seven times.



**Figure 4.** Effective intrinsic carrier concentration ( $n_{ieSiGe}$ ) at base-collector junction,  $n_{ieSiGe}(W_B)$  and base-emitter junction,  $n_{ieSiGe}(0)$  for  $y_E=0.01$  and varying  $y_C$  for three types of doping profiles.  $n_{ieSiGe}$  at  $x=0$  is same for three profiles

### 3.3. Diffusivity Profile

Figure 5 shows diffusivity for three base doping profiles at base-collector junction. Here  $y_E$  is fixed at 0.01 and  $y_C$  is varied. Diffusivity is observed by both considering and ignoring velocity saturation effect. For uniform doped base diffusivity has no significant changes while variation of  $y_C$ . Velocity saturation also has no significant effect on diffusivity for uniform profile.

For exponentially doped base diffusivity decreases

sharply with  $y_C$ . Velocity saturation effect is also greater for exponential doped base and no significant effect observed for Gaussian doped base. Due to increasing electric field with  $y_C$  at base collector junction and velocity saturation effect, electron mobility reduces in the base collector junction, as well as diffusivity reduces.

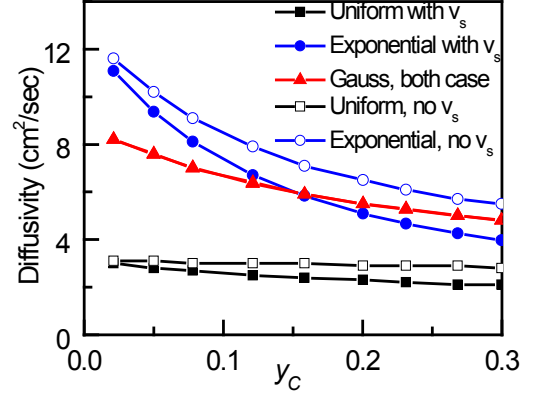


**Figure 5.** Diffusion coefficient at base-collector junction,  $D_{nSiGe}(W_B)$  for both considering velocity saturation effect and ignoring that for  $y_E=0.01$  and varying  $y_C$  for three types of doping profiles

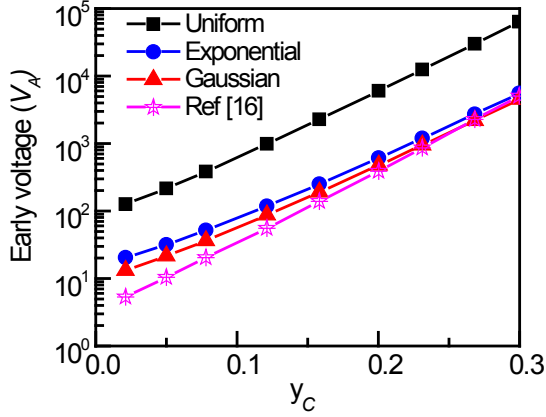
### 3.4. Early Voltage

Fig. 6 shows Early voltage for fixed  $y_E (=0.01)$  and varying  $y_C$  (0.01~0.3) for three types of base doping profiles. Early voltage for all three cases increases exponentially with  $y_C$ . Base width,  $W_B$  is 300 Å, peak doping at base-emitter junction is  $10^{19} \text{ cm}^{-3}$  and minimum doping at base-collector junction is  $10^{17} \text{ cm}^{-3}$  for Gaussian and exponential base profiles,  $10^{19} \text{ cm}^{-3}$  considered for uniform based doping profile.  $V_A$  for uniform doped base increases almost 500 times by increasing  $y_C$  from 0.01 to 0.3. For all three types of profiles  $V_A$  profile is similar. According to equation (2b) if effective intrinsic carrier concentration at the base-collector junction,  $n_{ieSiGe}(W_B)$  increases, it will increase Early voltage.  $n_{ieSiGe}(W_B)$  for uniformly doped base is greater than Gaussian and exponentially doped base (Fig. 4), so  $V_A$  for uniform doped base is greater than exponential and Gaussian doped base. It is also found that  $V_A$  is greater for exponential doped base than Gaussian doped base although  $n_{ieSiGe}(W_B)$  is same for both doping profiles. Actually Early voltage increases proportionally with the increase of  $n_{ieSiGe}(W_B)$ , but it has an inverse relation with total amount of  $n_{ieSiGe}$  content in the base (2b). Total amount of  $n_{ieSiGe}$  is greater for Gaussian than exponential doped base (Fig. 3a and Fig. 3b), and for this reason Early voltage is greater for exponential doping profile than Gaussian doping profile. Part of our Result (Gaussian doped base) compared with [16] and found in good agreement for  $V_A$ .

Figure 7 shows Early voltage for varying  $y_E$  with fixed  $y_C$  at 0.3. Here it is observed that by increasing  $y_E$ ,  $V_A$  reduces exponentially for three types of base doping profiles. While  $y_E$  is increased, this results in no variation in  $n_{ieSiGe}(W_B)$ , but it increases  $n_{ieSiGe}(0)$ , as well as  $n_{ieSiGe}$  throughout the base region. If  $n_{ieSiGe}$  at collector end ( $n_{ieSiGe}(W_B)$ ) is fixed but increases in the base region it will reduce  $V_A$  (equation 2a).



While  $y_E$  is nearly 0, this profile is triangular germanium profile,  $V_A$  in this profile is maximum, any other increment of  $y_E$  causes  $V_A$  reduces. When  $y_E=y_C=0.3$ , this shows box Germanium profile, in this case  $V_A$  is minimum.



**Figure 6.** Early Voltages for  $y_E=0.01$  and varying  $y_C$  for Gaussian, exponential and uniform base doping profiles. Base width,  $W_B$  is  $300\text{\AA}$ , peak doping at base-emitter junction is  $10^{19}\text{ cm}^{-3}$  and minimum doping at base-collector junction is  $10^{17}\text{ cm}^{-3}$  for Gaussian and exponential base profiles,  $10^{19}\text{ cm}^{-3}$  considered for uniform based doping profile. Triangular symbol used for Ref [16]

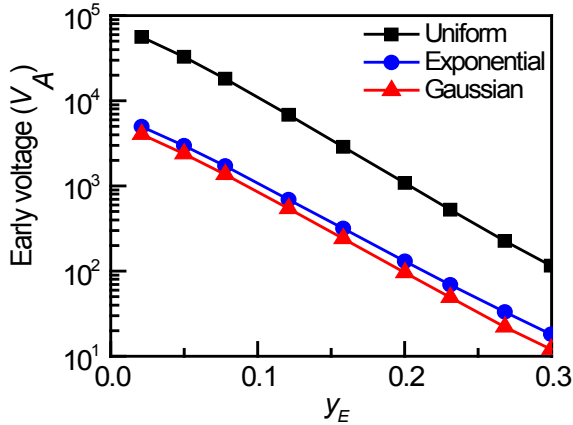


**Figure 7.** Early Voltage for  $y_C=0.3$  and varying  $y_E$  for Gaussian, exponential and uniform base doping profiles

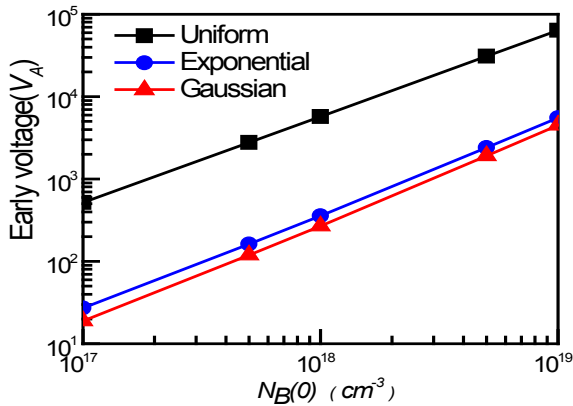


**Figure 8.** Early voltage ( $V_A$ ) for triangular germanium profile with  $y_C=0.3$  and  $y_E=0.01$  with varying base doping concentration. Doping concentration at base-collector junction for uniform doped  $N_B(W_B)=N_B(0)$  and for exponential and Gaussian doped  $N_B(W_B)=N_B(0)/100$

Figure 8 shows doping concentration dependency of  $V_A$

for three types of doping profiles, here it is observed that  $V_A$  is proportional to doping concentration. For exponential and Gaussian profiles for each  $N_B(0)$ ,  $N_B(0)/N_B(W_B)$  is kept constant at 100.

### 3.5. Collector Current Density ( $J_{CO}$ ) and Common Emitter Current Gain ( $\beta$ )

Figure 9 shows dependence of collector saturation current density ( $J_{CO}$ ) for uniform, exponential and Gaussian doped base with varying  $y_C$  and fixed  $y_E$  at 0.01.  $J_{CO}$  is considered for two cases, one is considering velocity saturation effect ( $v_s$ ) and another is ignoring that effect. For uniform doped base  $J_{CO}$  decreases with the increases of  $y_C$ . This decreasing of  $J_{CO}$  is true for both cases, either considering  $v_s$  or ignoring it. For exponential doped base if  $v_s$  is considered  $J_{CO}$  decreases, but otherwise it increases with  $y_C$ . It can be explained that for exponential doped base electron velocity reaches its saturation value before reaching base-collector junction. If we avoid  $v_s$  in our calculation, theoretically its velocity increase as well as  $J_{CO}$  also increases but if  $v_s$  is considered then electron velocity cannot overcome  $v_s$  and  $J_{CO}$  decreases. For Gaussian doped base  $v_s$  has no real impact on  $J_{CO}$ .

Collector current depends on quantity of intrinsic carrier concentration ( $n_{ie\text{SiGe}}$ ) as well as gradient of intrinsic carrier concentration ( $\Delta n_{ie\text{SiGe}}$ ) and diffusivity. The value of  $n_{ie\text{SiGe}}(0)$  and  $n_{ie\text{SiGe}}(W_B)$  for exponential doped base is same as  $n_{ie\text{SiGe}}(0)$  and  $n_{ie\text{SiGe}}(W_B)$  for Gaussian doped base respectively, but total amount of  $n_{ie\text{SiGe}}$  throughout the base is not same for these two profiles (Fig. 3a and Fig. 3b). The amount of  $n_{ie\text{SiGe}}$  is greater for Gaussian doped base, so  $J_{CO}$  is greater for Gaussian doped base than exponential doped base.

Electron mobility decreases when electric field increases (Fig. 5). Electric field increases exponentially as  $y_C$  increases (Fig. 2a and Fig. 2b) and electric field is maximum at the base-collector junction. As electric field for Gaussian doped base is higher than exponential doped base near base collector junction (Fig. 2b), so mobility for Gaussian doped base reduces at that junction as a result it cannot reach saturation value. For that reason  $v_s$  makes no real difference in  $J_{CO}$  for Gaussian doped base, but it has significant impact for uniform and exponential doped base.

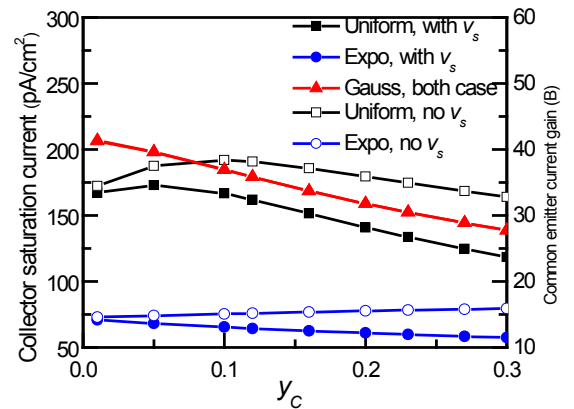


**Figure 9.** Collector saturation current density ( $J_{CO}$ ) for fixed  $y_E(0.01)$  and varying  $y_C$ . Right side of figure shows common emitter current gain ( $\beta$ ) considering  $J_{BO}=5\text{ pA/cm}^2$

**Table 1.** Calculated value showing current gain and Early voltage of SiGe HBT for various  $y_C$  and  $y_E$  combinations

| Mole fraction |       | Uniform |         | Exponential |         | Gaussian |         | Ref [10]-uniform |      |
|---------------|-------|---------|---------|-------------|---------|----------|---------|------------------|------|
| $y_E$         | $y_C$ | $V_A$   | $\beta$ | $V_A$       | $\beta$ | $V_A$    | $\beta$ | $V_A$            | $B$  |
| 0.01          | 0.01  | 18      | 111     | 379         | 39      | 11       | 39      |                  |      |
| 0.01          | 0.14  | 92      | 111     | 1937        | 29      | 64       | 35      |                  |      |
| 0.01          | 0.25  | 980     | 85      | 17446       | 24      | 643      | 30      |                  |      |
| 0.14          | 0.01  | 10      | 239     | 88          | 355     | 8        | 198     |                  |      |
| 0.14          | 0.14  | 15      | 803     | 378         | 256     | 11       | 357     | 18               | 750  |
| 0.14          | 0.25  | 137     | 1244    | 2880        | 202     | 89       | 312     | 120              | 1400 |
| 0.25          | 0.01  | 15      | 240     | -30         | 3551    | -4       | 309     |                  |      |
| 0.25          | 0.14  | 6       | 1730    | 122         | 3339    | 4        | 2769    | 6                | 1800 |
| 0.25          | 0.25  | 15      | 2300    | 378         | 2618    | 11       | 4213    | 44               | 1750 |

Figure 10 shows common emitter current gain ( $\beta$ ) for varying  $y_C$  and fixed  $y_E$  at 0.15. It can be observed that  $\beta$  increases up to certain limit of  $y_C$  for Gaussian and uniformly doped base after that it starts decreasing. For an *npn* transistor electron enters through emitter and major parts of it pass towards collector with negligible loss in base region due to electron hole recombination (which is out of this analysis). When  $y_C$  is small ( $\sim 0.01$ ) and  $y_E \sim 0.15$ , electron concentration is maximum near base-emitter junction and gradually decreases towards base-collector junction. While  $y_C$  increases electron concentration increases in the base-collector junction which causes collector saturation current as well as  $\beta$  to be increased. After certain  $y_C$  ( $\sim y_E$ ), electron concentration in collector-base junction is more than base-emitter junction which cause diffusion effect in the reverse direction to the normal electron flow from emitter to collector. Moreover diffusivity also reduces by increasing  $y_C$ . These two effects decrease collector saturation current as well as  $\beta$ . But for exponentially doped base  $\beta$  starts decreasing while  $y_C$  increases.

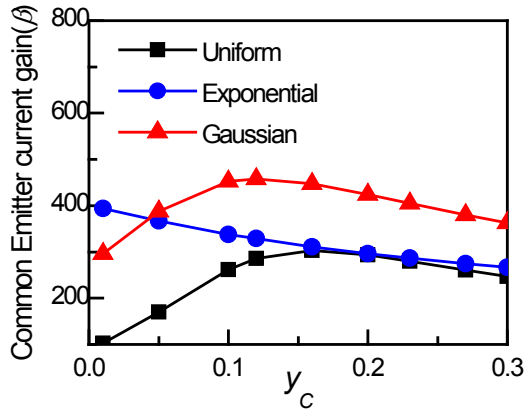
**Figure 10.** Common emitter current gain ( $\beta$ ) for  $y_E = 0.15$  and varying  $y_C$  for uniform, exponential and Gaussian doped base.  $J_{BO}$  is considered  $5 \text{ pA/cm}^2$ 

Table 1 shows calculated value of  $\beta$ ,  $V_A$  for 9 different devices containing various Germanium profiles at the base. For all these devices,  $J_{BO}$  was considered  $5 \text{ pA/cm}^2$ , base width ( $W_B$ ) is considered  $400 \text{ \AA}$ ,  $N_B(0)$  is considered  $10^{19} \text{ cm}^{-3}$ ,  $N_B(W_B)$  is  $10^{17} \text{ cm}^{-3}$  for Gaussian and exponentially doped

base. It is observed that for Gaussian and uniform doping profiles, if ( $y_C \geq y_E$ ) and ( $y_C - y_E$ ) increases by varying either  $y_C$  or  $y_E$ ,  $\beta$  decreases gradually but  $V_A$  increases. Conversely it can say that if ( $y_C \leq y_E$ ) and ( $y_E - y_C$ ) increases by varying either  $y_C$  or  $y_E$ ,  $\beta$  increases gradually but  $V_A$  decreases. Variation of  $\beta$  for trapezoidal and triangular germanium profiles can be explained by the above statements. For box germanium profile, increment of germanium has no significant change on  $V_A$ , but it increases  $\beta$  significantly. Increment of both  $y_C$  and  $y_E$  reduces diffusivity but it increases  $n_{ieSiGe}$  throughout the base region, which causes  $\beta$  to be increased for box germanium profile by increasing germanium content.

Part of this result (only uniform base doping profile with trapezoidal germanium profile) has been compared with [10]. Here it is found that  $V_A$  is in good match with [10] but some discrepancies found in  $\beta$  for higher  $y_C$  and  $y_E$ . Actually  $J_{BO}$  has considered fixed in the present analysis but its value was not same for all devices in [10].

## 4. Conclusions

In this work, an analytical model for Early voltage ( $V_A$ ) and common emitter current gain ( $\beta$ ) of Heterojunction Bipolar Transistor has been developed considering field dependent mobility, doping dependent mobility, band gap narrowing and velocity saturation effects. Dependences of Early voltage and common emitter current gain on different device parameter were studied. The results of the proposed models are compared with the data available in the literature found in good agreement. This analysis is important for optimum selection of various parameters for Early voltage and Common Emitter Current Gain of Heterojunction Bipolar Transistor.

## ACKNOWLEDGEMENTS

Authors of this paper would like to thank the Department of Electrical and Electronic Engineering (EEE), Bangladesh

University of Engineering and Technology (BUET), Dhaka-1000, Bangladesh, for its various supports during the course of this work.

## REFERENCES

- [1] N. Zerounian, F. Aniel, B. Barbalat, P. Chevalier, and A. Chantre, "500 GHz cutoff frequency SiGe HBTs", *Electronics Letters*, vol. 43, July 2007.
- [2] S. C. Jain, *Germanium-Silicon Strained Layers and Heterostructures*: Academic Press, Inc. USA, 1994.
- [3] M. K. Das, N. R. Das and P. K. Basu, "Effect of Ge content and profile in the SiGe base on the performance of a SiGe/Si HBT", *Microwave and Optical Technology Letters*, vol. 47, pp. 247-254, Nov 2005.
- [4] C. M. Krown and K. I. Anastasiou, "Early voltage in Heterojunction Bipolar Transistors: quantum tunneling and base recombination effects", *Solid State Electronics*, Vol. 38, pp. 1979-1991, 1995.
- [5] Z. R. Tang, T. Kamins and C. A. T. Salama, "Current Gain-Early Voltage Product in SiGe Base HBT's with Thin  $\theta$ -Si:H Emitters", *IEEE Tran. on Electron Devices*, pp. 473 - 476, 1994.
- [6] I. Tadao and Y. Yamauchi, "A Possible Near-Ballistic Collection in an AlGaAs/GaAs HBT with a Modified Collector Structure", *IEEE transactions on electron devices*, Vol. 35, No. 4, April 1988.
- [7] S. Y. Chiu and A. F. M. Anwar, "Effect of surface recombination on the Early voltage in HBTs", *Semicond. Sci. Technol*, Vol. 14, No. 9, September 1999.
- [8] Y. D. Wang, X. Yang and H. W. Zhang, "Effect of Base Structure Optimization of SiGe HBTs on Early Voltage", *Institute of Microelectronics, Tsinghua University, Beijing 100084, P.R. China*, 2006.
- [9] J. Ningyue and M. Zhenqiang, "Current gain of SiGe HBTs under high base doping concentrations", *Semicond. Sci. Technol*, Vol. 22, No. 1, January 2007.
- [10] E. J. Prinz and J. C. Sturm, "Current Gain-Early Voltage-Products in Heterojunction Bipolar Transistors with Non-uniform Base Bandgaps", *IEEE Electron Device Letters*, Vol. 12, No. 12, December 1991.
- [11] J. S. Yuan and J. Song, "Early voltage of SiGe Heterojunction Bipolar Transistor", *Electron Devices Meeting, IEEE Hongkong*, pp. 102-105, 1997.
- [12] C. J. Eduardo and F. P. Cortes, "Early Voltage and Saturation Voltage Improvement in Deep Sub-Micron Technologies Using Associations of Transistors", *SBCCI 08*, September 1-4, 2008, Gramado Brazil.
- [13] M. Domeij and H. S. Lee, "High Current Gain Silicon Carbide Bipolar Power Transistors", *International Symposium on Power Semiconductor Devices and IC's*, Naples, Italy, June 4-8, 2006.
- [14] M. J. Kumar and V. Parihar, "Surface Accumulation Layer Transistor (SALTran): A New Bipolar Transistor for Enhanced Current Gain and Reduced Hot-Carrier Degradation", *IEEE transactions on Device and Materials Reliability*, Vol. 4, No. 3, September 2004.
- [15] V. S. Patri and M. J. Kumar, "Profile Design Considerations for minimizing base transit time in SiGe HBT's", *IEEE Tran. on Electron Devices*, Vol. 45, pp. 1725-1731, Aug 1998.
- [16] A. Zareba, L. Lukasiak and A. Jakubowski, "The Influence of Selected Material and Transport Parameters on the Accuracy of Modeling Early Voltage in SiGe-Base HBT", *IEEE Transaction On Electron Devices*, Vol. 53, No. 8, August 2006.
- [17] J. A. Babcock, L. J. Choi, A. Sadovnikov, W. V. Noort, C. Estonilo, P. Allard, S. Ruby and G. Cestra, "Temperature interaction of Early voltage, current gain and breakdown characteristics of npn and pnp SiGe HBTs on SOI" *IEEE Bipolar/BiCMOS Circuits and Technology Meeting (BCTM)*, 2010.
- [18] J. A. Babcock, A. Sadovnikov, L. J. Choi, W. V. Noort, P. Allard and G. Cestra, "Forward and inverse mode Early voltage dependence on current and temperature for advanced SiGe-pnp on SOI" *IEEE Bipolar/BiCMOS Circuits and Technology Meeting (BCTM)*, 2011.
- [19] X. Xiao-Bo, Z. He-Ming, H. Hui-Yong and T. Q. Jiang, "Early effect of SiGe heterojunction bipolar transistors" *School of Microelectronics, Xidian University, Xi'an, Shaanxi, P. R. China*, 2012.
- [20] K. Suzuki and N. Nakayama, "Base transit time of shallow-base bipolar transistors considering velocity saturation at base-collector junction", *IEEE Trans. Electron Devices*, vol. 39, pp. 623-628, Mar. 1992.
- [21] J. D. Alamo, S. Swirhun and R. M. Swanson, "Simultaneous measurement of hole lifetime, hole mobility and bandgap narrowing in heavily doped n-type silicon", *IEDM Tech. Dig.*, pp. 290-293, 1985.
- [22] K. H. Kwok and C. R. Selvakumar, "Profile design considerations for minimizing base transit time in SiGe HBTs for all levels of Injection before onset of Kirk effect", *IEEE Tran. on Electron Devices*, vol. 48, pp. 1540-1549, 2001.
- [23] K. Suzuki, "Optimum base doping profile for minimum base transit time considering velocity saturation at base-collector junction and dependence of mobility and bandgap narrowing on doping concentration", *IEEE Tran. on Electron Devices*, vol. 48, pp. 2102-2107, 2001.
- [24] S. Basu, "Analytical modelling of base transit time of SiGe HBTs including effect of temperature", *International Semiconductor Conference, CAS'08*, vol. 2, pp. 339-342, Oct 2008.
- [25] S. T. Chang, C. W. Liu, and S. C. Lu, "Base transit time of graded-base Si/SiGe HBTs considering recombination lifetime and velocity saturation", *Solid-State Electron.*, vol. 48, pp. 207-215, 2004.
- [26] B. Y. Chen and J. B. Kuo, "An accurate knee current model considering quasi-saturation for BJTs operating at high current density", *Solid-State Electron.*, vol. 38, pp. 1282-1284, Jun 1995.
- [27] A. Zareba, L. Lukasiak, and A. Jakubowski, "Modeling of SiGe-base heterojunction bipolar transistor with gaussian doping distribution", *Solid-State Electron.*, vol. 45, pp. 2029-2032, 2001.
- [28] J. W. Slotboom and H. C. d. Graaff, "Measurement of bandgap narrowing in Si bipolar transistors", *Solid-State Electron.*, vol. 19, pp. 857-862, 1976.
- [29] H. Kroemer, "Two integral relations pertaining to electron transport through a bipolar transistor with a nonuniform energy gap in the base region", *Solid-State Electron.*, vol. 28, pp. 1101-1103, 1985.